J Therm Anal Calorim (2012) 107:471–475
DOI 10.1007/s10973-011-1454-4

Study on thermal decomposition of copper(II) acetate monohydrate in air

Zhenkun Lin · Donglin Han · Shufen Li

Received: 11 January 2011 / Accepted: 7 March 2011 / Published online: 18 March 2011

Abstract The thermal decomposition of copper(II) acetate monohydrate ($CuAc_2{\cdot}H_2O$) under 500 °C in air was studied by TG/DTG, DTA, in situ FTIR and XRD experiments. The experimental results showed that the thermal decomposition of $CuAc_2{\cdot}H_2O$ under 500 °C in air included three main steps. $CuAc_2{\cdot}H_2O$ was dehydrated under 168 °C; $CuAc_2$ decomposed to initial solid products and volatile products at 168–302 °C; the initial solid products Cu and Cu_2O were oxidized to CuO in air at 302–500 °C. The copper acetate peroxides were found to form between 100 and 150 °C, and the dehydration of these peroxides resulted in the presence of $CuAc_2{\cdot}H_2O$ above 168 °C. The initial solid products were found to be the admixture of Cu, Cu_2O, and CuO, not simply the single Cu_2O as reported before. Detailed reactions involved in these three steps were proposed to describe the complete mechanism and course of the thermal decomposition of $CuAc_2{\cdot}H_2O$ in air.

Keywords Copper(II) acetate monohydrate · Thermal decomposition · Dehydration · Oxidation · Peroxides

Introduction

Thermal decomposition and dehydration of metal acetates have been studied broadly under various conditions [1–20]. As a typical and widely applied metal acetate, the thermal decomposition of copper(II) acetate monohydrate ($CuAc_2{\cdot}H_2O$) has attracted special attention in the past 20 years and many valuable experimental conclusions were obtained. Afzal et al. [3] concluded that the decomposition of the anhydrous copper acetate ($CuAc_2$) after the dehydration yielded Cu, CH_3COOH, CO_2, C, and H_2. Mansour [10] indicated that $CuAc_2{\cdot}H_2O$ was dehydrated at 190 °C and then partially decomposed at 220 °C giving rise to CuO in addition to a minor portion of Cu_2O and Cu_4O_3. Zhang et al. [15] found that the thermal decomposition of $CuAc_2{\cdot}H_2O$ occurred in four steps in air, and the dehydration reaction contained an initial reversible step and two other irreversible steps.

Many conclusions reported in the above references disagree with each other, therefore, continuous and in-depth studies about the thermal decomposition of $CuAc_2{\cdot}H_2O$ are greatly necessary and important. In this work, the thermal decomposition behaviors and products of $CuAc_2{\cdot}H_2O$ in air atmosphere are studied by TG/DTG, DTA, in situ FTIR, and XRD. The decomposition intermediates are specially attended in this work so that complete mechanism and course of the thermal decomposition of $CuAc_2{\cdot}H_2O$ in air can be propounded and discussed.

Experimental

Sample

$CuAc_2{\cdot}H_2O$ was supplied by Sinopharm Chemical Reagent Co., Ltd, Shanghai, China, the particle size was lower than 160 μm.

Z. Lin (✉)
Institute of Watershed Science and Environmental Ecology,
Wenzhou Medical College, Wenzhou 325035,
People's Republic of China
e-mail: zklin@wzmc.edu.cn

D. Han · S. Li
Department of Chemical Physics, University of Science
and Technology of China, Hefei 230026,
People's Republic of China

Instrumental

Simultaneous TG/DTG and DTA measurements were carried out using a Shimadzu DTG-60H Thermal Analyzer. The experiments were performed in flowing air atmosphere (flow rate = 40 mL/min) with the heating rate of 10 °C/min. The sample weight was about 8 mg.

In situ Fourier transform infrared (in situ FTIR) spectra were recorded by a Nicolet MAGNA-IR 750 spectrometer using KBr pellets with the spectral range of 4000–500 cm^{-1} in air atmosphere.

XRD experiments of the solid decomposition products of $CuAc_2 \cdot H_2O$ were carried out on an MXPAHF 18 kW rotating anode X-Ray diffractometer (MaxScience, Japan) with a level goniometer. The powder XRD patterns were recorded within the 2θ range of 10–70° using Cu Kα1 radiation ($\lambda = 0.154056$ nm, 40 kV, 100.0 mA, 8.000°/min). Samples of $CuAc_2 \cdot H_2O$ were heated to the desired temperature (110, 210, 310, 410, and 510 °C) with the heating rate of 10 °C/min in air, and then the solid decomposition products were stored in sealed containers, preparing for XRD experiments. The samples for XRD experiments were named $CuAc_2 \cdot H_2O(x)$, in which x denoted the end temperature of decomposition.

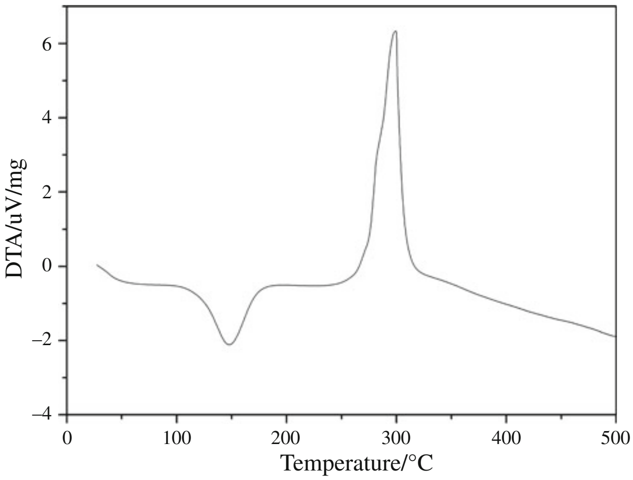

Fig. 2 DTA curve for thermal decomposition of $CuAC_2 \cdot H_2O$ in air

Table 1 Mass changes of $CuAc_2 \cdot H_2O$ thermal decomposition in air

Step	Temperature range/°C	Mass change/%
1	106–168	−9.88
2	168–302	−55.79
3	302–400	2.45

Results and discussion

TG/DTG and DTA curves of $CuAc_2 \cdot H_2O$ are shown in Figs. 1 and 2, respectively. The TG/DTG curves display two mass loss steps and one mass increase step in the temperature range from 30 to 500 °C in air, and the corresponding data of mass changes are list in Table 1.

Generally, the two mass loss steps were attributed to dehydration of $CuAc_2 \cdot H_2O$ and decomposition of $CuAc_2$, respectively, while the mass increase step was attributed to oxidation of solid decomposition products like Cu_2O and Cu_4O_3 [10, 15]. Table 1 shows that experimental value of first mass loss step is higher than the theory value (9.02%) of absolute dehydration of $CuAc_2 \cdot H_2O$. This indicates that other events, which result in mass loss, occur in this temperature range (106–168 °C). The $CuAc_2$ on the surface of the sample is possibly oxidized and some kind of $CuAc_2$ peroxides form in air. These peroxides are instable and begin to decompose at low temperature (under 168 °C), resulting in farther mass loss at 106–168 °C besides the dehydration of $CuAc_2 \cdot H_2O$. The forming and decomposition of the $CuAc_2$ peroxides may disturb the dehydration process of $CuAc_2 \cdot H_2O$, therefore, two near but separate steps of dehydration were observed in air [10, 15, 16].

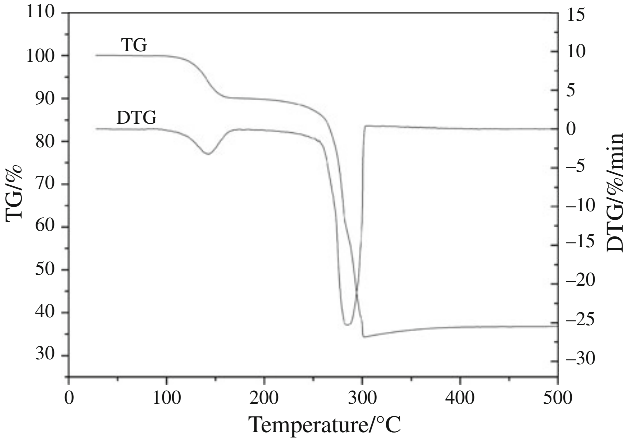

Fig. 1 TG and DTG curves for thermal decomposition of $CuAc_2 \cdot H_2O$ in air

Figures 1 and 2 do not show two steps of the dehydration process owing to the factors of experimental instrumentals and condition, however, the forming of $CuAc_2$ peroxides is effectively supported by the in situ FTIR experimental results below. The similar phenomenon was also observed in nitrogen atmosphere [10]. Because the forming of $CuAc_2$ peroxides required only a small quantity of oxygen and the impure nitrogen which contained a little oxygen was adopted. The forming of the $CuAc_2$ peroxides is a mass increasing and heat releasing process, which is consistent with the reported DTG and DTA curves [10, 16].

The second mass loss step was commonly supposed to the decomposition of $CuAc_2$ and the formation of Cu_2O

since the experimental value of the mass loss for this step was close to the theory value (−55.10%) [15]. However, the above supposition does not accord with the result of TG experiment in this work. Though the experimental value of the mass loss showed in Table 1 is close to −55.10%, the mass increase between 302 and 400 °C is much lower than the theory value (4.0%) of Cu_2O oxidizing to CuO. The solid products formed under 302 °C are possibly the admixture of Cu_2O, CuO, and Cu, not simply the single Cu_2O. This supposition is evidently supported by the results of XRD experiment below.

The in situ FTIR spectra from room temperature (RT) to 400 °C are showed in Fig. 3, and the assignments of the absorptive peaks are listed in Table 2. The FTIR spectra in Fig. 3 show that $CuAc_2{\cdot}H_2O$ begins to be dehydrated between 100 and 150 °C, which is consistent with the TG/DTG and DTA results. The absorptive peaks of crystal water around 3380 cm^{-1} distinctly weaken at 150 °C, and simultaneously new peaks at 3520 cm^{-1} and 1000–700 cm^{-1} appear. Some of these new absorptive peaks are ascribed to the peroxides as it showed in Table 2. These evidences show that peroxides of $CuAc_2$ form between 100 and 150 °C, which accords with the result of TG/DTG experiment above.

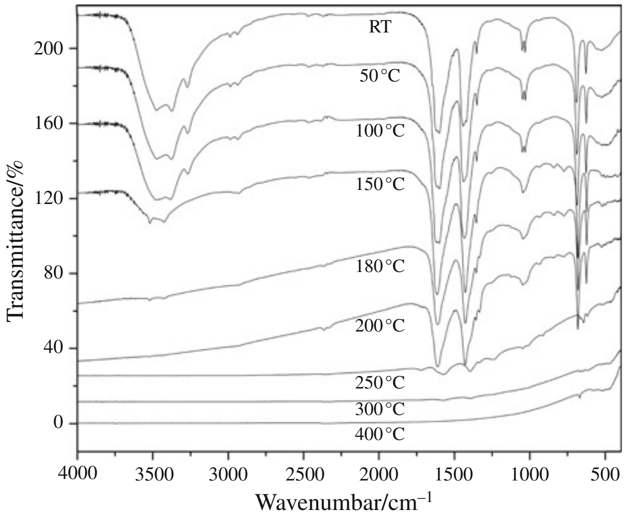

Fig. 3 In-situ FTIR spectra for the solid products of $CuAc_2{\cdot}H_2O$ thermal decomposition in air

Table 2 Assignments of the FTIR spectra in Fig. 3

Wavenumber/cm^{-1}	Assignment
3520[a]	O–H stretching in acetic acid or peroxides
3380	O–H stretching in crystal water
2990	C–H stretching in methyl
2940	C–H stretching in methyl
1602	C=O stretching
1442	C=O stretching, C–H bending in methyl
1353	C–H bending in methyl
1051	C–CH_3 framework vibration
1034	C–CH_3 framework vibration
1050[a]	C–O stretching in peroxides
840[a]	O–O stretching in peroxides
690	Acetate anion scissoring
629	Acetate anion twisting

[a] Not detected in room temperature

The FTIR spectra in Fig. 3 show that the absorptive peaks around 3380 cm^{-1} disappear at 180 °C, which reveals that the dehydration of $CuAc_2{\cdot}H_2O$ finishes between 150 and 180 °C. The absorptive peaks at 1602 and 1442 cm^{-1} both distinctly weaken at 250 °C and disappear at 300 °C, which reveals that $CuAc_2$ begins to decompose between 200 and 250 °C and finishes under 300 °C. The above results from the FTIR spectra accord well with the results of TG/DTG and DTA experiments. The FTIR spectra also show that the decomposition of peroxides finishes before 250 °C, revealing that these peroxides are unstable like other peroxides.

XRD profiles of $CuAc_2{\cdot}H_2O$ (110, 210, 310, 410, and 510 °C) are showed in Fig. 4. The XRD profiles display that $CuAc_2{\cdot}H_2O$ is steady under 110 °C and no decomposition products is detected, and this is consistent with the results of TG/DTG, DTA, and in situ FTIR experiments. $CuAc_2{\cdot}H_2O$ and $CuAc_2$ are both observed in the XRD profile of $CuAc_2{\cdot}H_2O$(210). The presence of metal acetates like nickel acetate tetrahydrate after dehydration was ascribed to the remaining crystal water [10]. However, this explanation is not reasonable for the presence of $CuAc_2{\cdot}H_2O$ after dehydration as the TG/DTG, DTA, and in situ FTIR experiments above show that dehydration of $CuAc_2{\cdot}H_2O$ is completed in much lower temperature than 210 °C and the water from dehydration should have escaped from the sample before. The presence of $CuAc_2{\cdot}H_2O$ at 210 °C is possibly resulted in the combination of $CuAc_2$ and the H_2O from the dehydration of the $CuAc_2$ peroxides [20].

Figure 4 shows that the decomposition of $CuAc_2$ finishes before 310 °C as the XDR peaks of $CuAc_2$ disappear in the XRD profile of $CuAc_2{\cdot}H_2O$(310). TG/DTG and DTA curves above show that $CuAc_2$ finishes decomposition at about 310 °C, as a result, Cu, Cu_2O, and CuO which are detected in $CuAc_2{\cdot}H_2O$(310) should be the initial solid products of $CuAc_2$. This conclusion is supported by the results of TG/DTG and DTA experiments. It can be known from the XRD profiles in Fig. 4 that the contents of Cu and Cu_2O decrease gradually, while the content of CuO increases gradually from 310 to 510 °C. This reveals that Cu and Cu_2O are gradually oxidized to CuO in air. It can be known from the XRD profile of $CuAc_2{\cdot}H_2O$(510) that all Cu have been oxidized to CuO while a small quantity of Cu_2O remains in the solid products of $CuAc_2{\cdot}H_2O$ thermal decomposition at 510 °C in air.

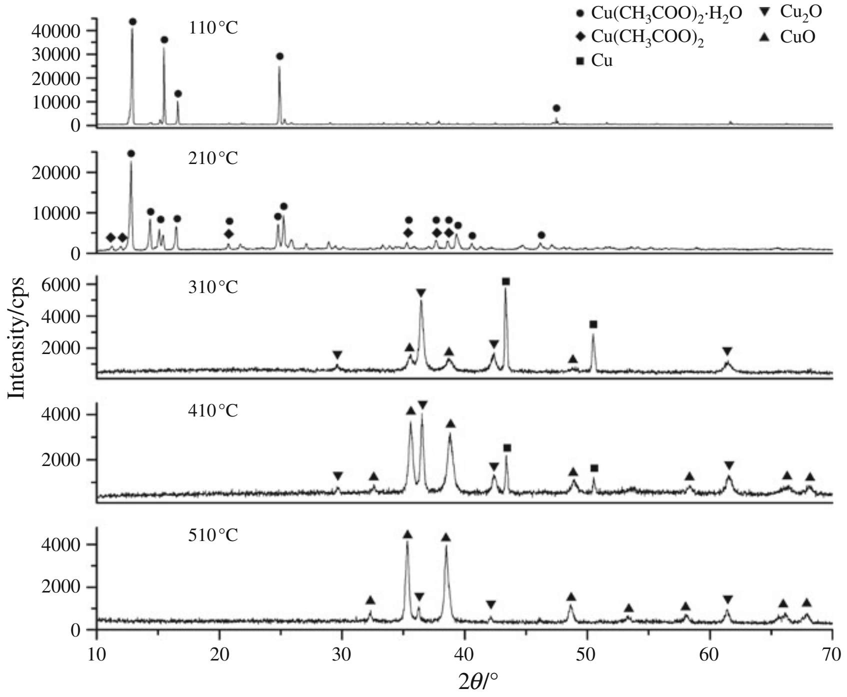

Fig. 4 XRD profile for the solid products of $CuAc_2·H_2O$ thermal decomposition in air

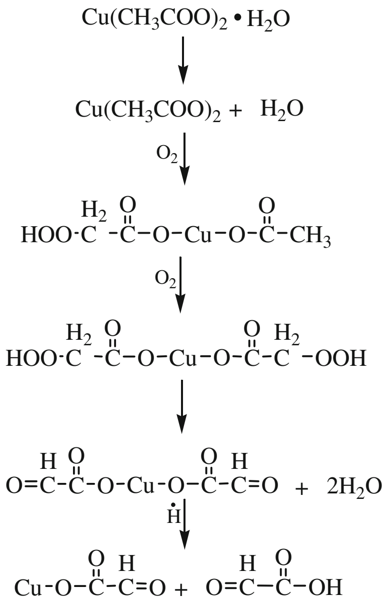

Scheme 1 Reactions involved in the first step of thermal decomposition of $CuAc_2·H_2O$ in air

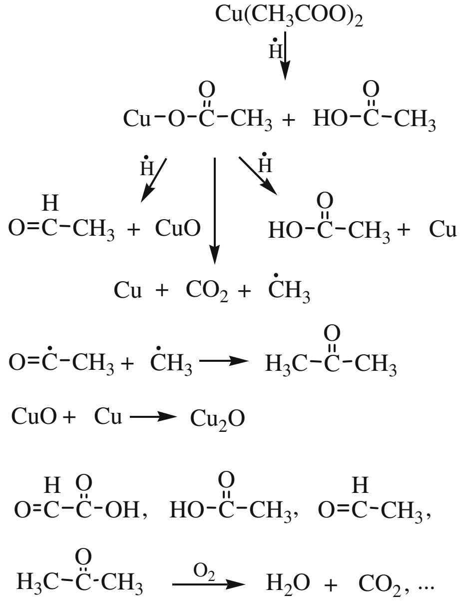

Scheme 2 Reactions involved in the second step of thermal decomposition of $CuAc_2·H_2O$ in air

$$Cu \xrightarrow{1/2\,O_2} CuO \qquad Cu_2O \xrightarrow{1/2\,O_2} 2\,CuO$$

Scheme 3 Reactions involved in the third step of thermal decomposition of $CuAc_2·H_2O$ in air

Basing on the results of TG/DTG, DTA, in situ FTIR, and XRD experiments above, it may be suggested that the thermal decomposition of $CuAc_2·H_2O$ under 500 °C in air includes three main steps. The involved reactions are showed in Schemes 1, 2, and 3, respectively, corresponding to the three decomposition steps.

In the first step (under 168 °C), $CuAc_2·H_2O$ is dehydrated and a small quantity of $CuAc_2$ is oxidized to $CuAc_2$ peroxides under 168 °C as it showed in Scheme 1. These $CuAc_2$ peroxides are also dehydrated and decompose to smaller products including volatile products, leading to the extra mass loss besides dehydration of $CuAc_2·H_2O$ as the result of TG/DTG experiment shows above. Note that the dehydration and decomposition of the $CuAc_2$ peroxides may last until above 168 °C. The presence of $CuAc_2·H_2O$ at higher temperature is possibly due to the combination of $CuAc_2$ and the H_2O from dehydration of the $CuAc_2$ peroxide as mentioned above.

In the second step (168–302 °C), $CuAc_2$ decomposes to small volatile products and the volatile products are oxidized by the oxygen in air. The volatile products acetic acid, acetaldehyde, acetone, and CO_2 in Scheme 2 have been detected in the decomposition of $CuAc_2·H_2O$ or cobalt acetate tetrahydrate [3, 10]. The initial solid products Cu, Cu_2O, and CuO also form in this step.

In the third step (302–500 °C), the solid products Cu and Cu_2O are oxidized to CuO in air as it showed in Scheme 3.

Some important results, which have not been reported before, were obtained in this work. The $CuAc_2$ peroxides were identified, which made the dehydration of $CuAc_2·H_2O$ separate to two steps and resulted in the presence of $CuAc_2·H_2O$ after dehydration. The initial solid products were found to be the admixture of Cu, Cu_2O, and CuO, not the single Cu_2O as reported before. The observed experimental results can be explained well by the proposed reactions in Schemes 1, 2, and 3, and these reactions can describe the whole course of the thermal decomposition of $CuAc_2·H_2O$ under 500 °C in air.

Conclusions

The thermal decomposition of $CuAc_2·H_2O$ under 500 °C in air includes three main steps. $CuAc_2$ peroxides form during the dehydration of $CuAc_2·H_2O$, and the dehydration of these peroxides result in the presence of $CuAc_2·H_2O$ above 168 °C. The initial solid decomposition products of $CuAc_2·H_2O$ are the admixture of Cu, Cu_2O, and CuO. Cu and Cu_2O are oxidized to CuO in air as the temperature increases. The proposed detailed reactions for the purpose of describing complete course of the thermal decomposition of $CuAc_2·H_2O$ in air, can explain the observed experimental results well.

Acknowledgements We greatly appreciate the financial support provided by the National Natural Science Foundation of China (50476025) and Research Foundation for Talents of Wenzhou Medical College (QTJ09020).

References

1. Koga N, Tanaka H. Kinetic study of the thermal dehydration of copper (II) acetate monohydrate I. Single crystal material. Solid State Ionics. 1990;44:1–9.
2. Tanaka H, Koga N. Kinetic study of the thermal dehydration of copper(II) acetate monohydrate II. Crushed crystals. Thermochim Acta. 1990;173:53–62.
3. Afzal M, Butt PK, Ahmad H. Kinetics of thermal decomposition of metal acetates. J Therm Anal. 1991;37:1015–23.
4. Diefallah EM. Kinetic analysis of thermal decomposition reactions: Part VI. Thermal decomposition of manganese(II) acetate tetrahydrate. Thermochim Acta. 1992;202:1–16.
5. Mohamed MA, Halawy SA, Ebrahim MM. Non-isothermal decomposition of nickel acetate tetrahydrate. J Anal Appl Pyrol. 1993;27:109–18.
6. Mohamed MA, Halawy SA, Ebrahim MM. Non-isothermal kinetic and thermodynamic study of the decomposition of lead acetate trihydrate. Thermochim Acta. 1994;236:249–62.
7. Mohamed MA, Halawy SA. Kinetic and mechanistic study of the non-isothermal decomposition of manganese(II) acetate tetrahydrate. Thermochim Acta. 1994;242:173–86.
8. Ball MC, Portwood L. The dehydration of copper(II) acetate monohydrate. J Therm Anal. 1994;41:347–56.
9. Mohamed MA, Halawy SA, Ebrahim MM. The non-isothermal decomposition of cobalt acetate tetrahydrate: a kinetic and thermodynamic study. J Therm Anal. 1994;41:387–404.
10. Mansour SAA. Thermoanalytical investigations of the decomposition course of copper oxysalts III. Copper(II) acetate monohydrate. J Therm Anal. 1996;46:263–74.
11. Obaid AY, Alyoubi AO, Samarkandy AA, Al-Thabaiti SA, Al-Juaid SS, El-Bellihi AA, Deifallah EM. Kinetics of thermal decomposition of copper(II) acetate monohydrate. J Therm Anal Calorim. 2000;61:985–94.
12. Zhang KL, Jia MK, Tang H, Guo GH. The thermal decomposition mechanism of cobaltous acetate. J Wuhan Univ (Nat Sci Ed). 2002;48:409–12.
13. Ghule AV, Ghule K, Chen CY, Chen WY, Tzing SH, Chang H, Ling YC. In situ thermo-TOF-SIMS study of thermal decomposition of zinc acetate dehydrate. J Mass Spectrom. 2004;39:1202–8.
14. Jesus JCD, González I, Quevedo A, Puerta T. Thermal decomposition of nickel acetate tetrahydrate: an integrated study by TGA, QMS and XPS techniques. J Mol Catal A Chem. 2005;228:283–91.
15. Zhang KL, Hong JH, Cao GH, Zhan D, Tao YT, Cong CJ. The kinetics of thermal dehydration of copper(II) acetate monohydrate in air. Thermochim Acta. 2005;437:145–9.
16. Ren N, Zhang XF, Bai JH, Zhang JJ. Study on thermal decomposition kinetics of copper acetate dihydrate with popescu method. J Hebei Norm Univ (Nat Sci Ed). 2005;29:584–7.
17. Logvinenko V, Polunina O, Mikhailov Y, Mikhailov K, Bokhonov B. Study of thermal decomposition of silver acetate. J Therm Anal Calorim. 2007;90:813–6.
18. Lin CC, Li YY. Synthesis of ZnO nanowires by thermal decomposition of zinc acetate dehydrate. Mater Chem Phys. 2009;113:334–7.
19. Bakrania SD, Rathore GK, Wooldridge MS. An investigation of the thermal decomposition of gold acetate. J Therm Anal Calorim. 2009;95:117–22.
20. Mu GZ. Reaction of free radical. Beijing: Higner Education Press; 1985.